Available online at www.sciencedirect.com
ScienceDirect
Journal of Nuclear Materials 372 (2008) 239–248
journal of nuclear materials
www.elsevier.com/locate/jnucmat

Interaction of a single interstitial atom with small clusters of self interstitials in α-Fe

N. Anento, A. Serra *

Departament de Matemàtica Aplicada III, Escola d'Enginyeria de Camins, Unversitat Politècnica de Catalunya, Jordi Girona 1-3, 08034 Barcelona, Spain

Received 8 August 2006; accepted 21 March 2007

Abstract

The interaction of a self-interstitial atom (SIA) with small clusters (7 and 19 SIAs) in α-Fe has been studied by atomic computer simulation using an interatomic potential of EAM type derived by Ackland et al. Metastable configurations have been investigated by annealing the system at 50 K and 100 K. The interstitial exhibits six non-equivalent configurations that lead to different behaviour under the stress field of the cluster. Special configurations, formed when the SIA joins the cluster, that prevent cluster motion are described. The region where the interstitial is attracted to and joins the cluster and the binding energy map are presented. The capture distance and recombination energy of a vacancy interacting with the same clusters, calculated with the same potential, is given for comparison.

PACS: 61.72.Ji; 61.72.Yx

1. Introduction

Planar clusters of point defects and dislocation loops formed from self-interstitial atoms (SIAs) are created directly in high-energy displacement cascades in metals under irradiation [1–3]. They play an important role in the microstructure evolution and directly affect the change of mechanical properties [4] since they can form specific microstructures, i.e., rafts of dislocation loops and dislocation decoration [5]. The processes of growth and shrinkage of clusters created in cascades is directly related to the interaction with point defects. The first step for a comprehensive study of the cluster capture efficiency of such point defects is the description of the structure, stress field and mobility of clusters, and the corresponding interaction energies. The structure, stress field and mobility of SIA clusters bigger than 7 SIAs have been extensively studied [6–8] (see Section 3) and the interaction between a vacancy and a cluster has been studied by both computer simulation and elasticity theory up to clusters of 127 SIAs [9]. It was revealed that the interaction at short distances cannot be described by the elasticity theory. Moreover, for clusters of 19 SIAs or bigger the annihilation of the vacancy is produced only with the interstitials of the periphery.

The interaction of a cluster with an SIA is more complex since SIAs are anisotropic defects that exhibit six orientations that are not equivalent in the presence of a stress field such as the one created by the cluster. For a better understanding of the cluster interaction with interstitials it follows some considerations on the relative motion of these defects. An interstitial migrates by a translation–rotation motion to the nearest lattice site (Johnson mechanism), i.e., it changes site and orientation, which compares with a single jump of the vacancy. SIA clusters are highly mobile. Clusters of 5 SIAs or more have a thermally activated 1D motion in the [1 1 1] crowdion direction. This implies that the interactions take place in the vicinity of the cluster glide prism; therefore, for a reaction to occur, point defects that perform 3D random walk should either be near the glide prism or go there. For a given temperature, the diffusion coefficients of the defects are ordered

* Corresponding author. Fax: +34 934011825.
E-mail address: a.serra@upc.edu (A. Serra).

0022-3115/$ - see front matter © 2007 Elsevier B.V. All rights reserved.
doi:10.1016/j.jnucmat.2007.03.230

as follows: D(cluster) $\geqslant$ D(interstitial) $\gg$ D(vacancy). As a consequence, during the time scale of the interaction the vacancy can be considered immobile and it is the cluster that glides towards the vacancy when the latter is located inside the cluster glide prism [9,10]. In the case of the interaction with interstitials both defects move under their mutual interaction. This difference in the kinetics of point defects may be determinant in the final balance of the capture efficiency. Another significant difference with the interaction with vacancies, which are centres of negative dilatation to a first approximation, is that the attraction or repulsion of an SIA cannot be related directly to the pressure created by the cluster since, for a given SIA site, the interaction is a function of the orientation of the interstitial and may be attractive or repulsive. Consequently, for the determination of the effective capture volume of SIA clusters, a detailed calculation by computer simulation of the cluster–SIA binding energy is necessary.

In this paper we describe the interaction of small SIA clusters (7 and 19 SIAs) with a self-interstitial atom as a function of the relative position of the interstitial and its orientation. The capture volume for the spontaneous absorption is deduced and a comparison with the corresponding values for the interaction with a vacancy is given. These results are the necessary input for a Monte Carlo study of the capture efficiency of clusters for point defects. This work is now in progress.

2. Computational method and notation

2.1. Simulation procedure

Atomic-scale computer simulation has been used both in the form of static relaxation (potential energy minimization) and molecular dynamics (MD). The system studied contained approximately 400 000 mobile atoms. The box was elongated along the Z-axis coincident with the [1 1 1] crystallographic direction, namely the cluster Burgers vector.

The interatomic interaction was described by an EAM-type many-body potential parameterized by Ackland et al. [11] for α-Fe that ensures a reasonable description of atomic interactions at small separations, i.e., stable ⟨1 1 0⟩ dumbbell orientation for a single self-interstitial atom with a formation energy, $E_f^I = 3.59$ eV, in a reasonable agreement with first principle calculations (3.64 eV, [12]).

Initially, an isolated cluster was created in the centre of the crystal and relaxed to the minimum of the potential energy. An interstitial was then inserted at a chosen position and orientation and the system was relaxed again using a combination of conjugate gradients and quasi-dynamic relaxation [13] until the final mean gradient per atom was reduced to $\sim 10^{-8}$ eV/a_0 (a_0 is the lattice parameter). After the final relaxation the cluster–interstitial binding energy was estimated and the configuration was investigated. The binding energy is defined as $E^b =$

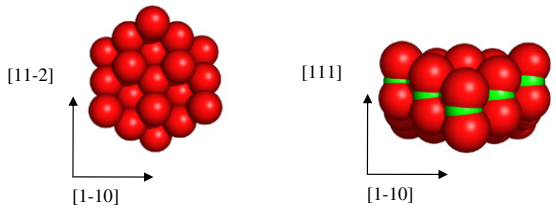

Fig. 1. Two views of a relaxed 19 SIAs cluster, each interstitial is represented by a vacancy (light sphere) and two atoms (dark spheres). The left view is along the [1 1 1] crowdion direction. Notice the hexagonal shape of the cluster (left) and the three positions of the interstitials within the cluster habit plane (1 1 1).

E^f(cluster) + E^f(SIA) − E^f(cluster + SIA), where E^f is the formation energy.

The stability of some configurations was tested by annealing the system at 50 K and/or 100 K up to 2 ns. In the relaxed configuration the position of all the interstitials was analysed and an interstitial atom was identified as two atoms in the same Wigner–Seitz cell. Then the cluster and interacting interstitial were viewed using molecular-modelling software PyMOL [14]. In the images each dumbbell or crowdion interstitial is represented by two atoms and a vacancy in between, the latter located in the lattice site of the reference perfect crystal as shown in Fig. 1. Notice the hexagonal shape of the cluster and the three levels of the interstitials in the (1 1 1) plane.

2.2. Notation used to describe the position of the interstitial relative to the cluster

A ⟨1 1 0⟩ dumbbell has six possible orientations which are equivalent in an otherwise perfect crystal. On introducing a cluster the symmetry of the interstitial surroundings is broken and these orientations are no longer equivalent, therefore the binding energy has to be studied for each of them. Fig. 2 shows two groups of interstitial orientations:

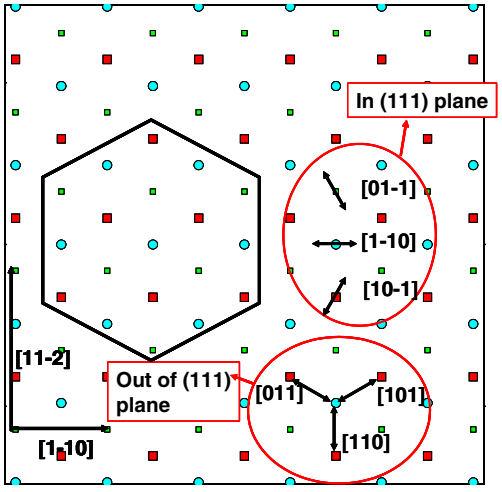

Fig. 2. Scheme of the cluster represented by the hexagon and the six orientations of the interstitial, three in the (1 1 1) plane and three out of the (1 1 1) plane. X and Y axes of reference are indicated at the left.

three parallel to the cluster habit plane [0 1 −1], [1 −1 0], [1 0 −1] ('inplane' hereafter) and three forming an angle with the cluster habit plane [0 1 1], [1 1 0], [1 0 1] ('outplane').

Notice that [1 −1 0] and [1 1 0] are invariant under a rotation of 180° about the [1 −1 0] axis whereas [1 0 −1] and [1 0 1] transform to [0 1 −1] and [0 1 1], respectively, by the same rotation. This reduces the study of the interaction to one side of the cluster habit plane. Thus, the results obtained for the [1 0 −1] orientation in one side of the cluster are coincident with the results obtained for [0 1 −1] on the other side and vice versa.

In Fig. 3(a) (1 1 1) cross section of the crystal containing the SIA clusters is presented, where the cluster location is indicated by the hexagon. The reference system used to indicate the position of the interstitial is $\{X = [1\,-1\,0]; Y = [1\,1\,-2]; Z = [1\,1\,1]\}$. The cluster is in the plane $z = 0$ and it is centred at the origin. The units along the axes are taken as the interplanar distances, i.e., $\sqrt{2}/2a_0$, $\sqrt{6}/4a_0$ and $\sqrt{3}/6a_0$. In this way a position of the lattice site in the plane of the cluster is indicated as shown in Fig. 3. Each point in the shadowed triangle represents the position of the [1 1 1] lines (perpendicular to the cluster habit plane) where the binding energy has been calculated. The interstitial has been located at each crystal site along these lines, namely at positions separated by $\Delta z = 3(\sqrt{3}/6)a_0$, and then the system has been relaxed to its minimum energy.

The [1 1 1] lines studied are grouped according to their positions (see Fig. 3) in two sets, namely, the lines *inside* the glide prism: (0 0 0), (1 1 1) and (1 −1 −1) for 7 SIAs and 19 SIAs clusters, plus (2 0 0), (2 2 −1) and (2 −2 1) for the 19 SIAs cluster; and the lines *outside* the glide prism. The latter are grouped, in turn, in first neighbour, second neighbour and third neighbour lines. Thus, the notation '19 SIAs (2 −2 1)' corresponds to a line inside the glide prism whereas '7 SIAs (2 −2 1)' corresponds to a line in the first neighbour position outside the glide prism.

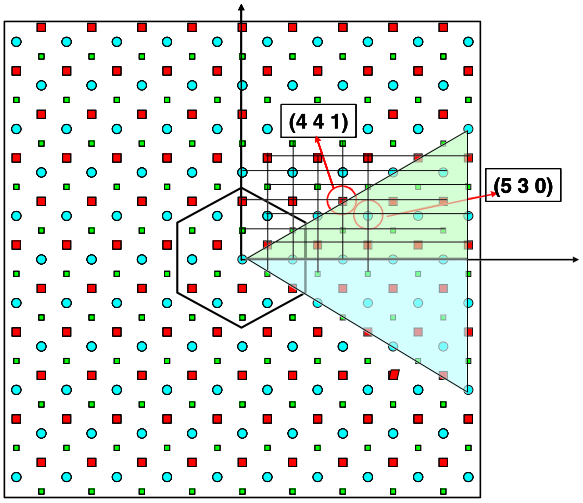

Fig. 3. The shadowed triangle is the projection on the cluster habit plane of the studied region. The grid has been included to understand the notation used for the identification of the [1 1 1] lines where the interstitial is located.

3. Description of a single interstitial and self-interstitial clusters

3.1. Self-interstitial atom

SIAs in α-Fe are stable as dumbbells in the ⟨1 1 0⟩ orientation with formation energy, with the model potential used, $E_F = 3.59$ eV. These are very anisotropic defects as compared with vacancies. Fig. 4 shows the pressure distribution across the (0 0 1) plane that contains the interstitial. Interstitials in Fe perform a 3D migration. The static migration energy barrier of an interstitial in the bulk depends on the migration mechanism. Ab initio calculations [15,16] have shown that the smaller barrier corresponds to the Johnson mechanism, namely translation and rotation. Therefore, when an interstitial jumps to a neighbouring position it changes its orientation. The value of the migration energy barrier in the bulk calculated with the EAM potential is $E_m = 0.31$ eV, compared with 0.34 eV from ab initio.

3.2. Self-interstitial clusters

Although single SIAs in iron are stable as dumbbells in the ⟨1 1 0⟩ orientation, clusters formed by more than four interstitials are more stable in the ⟨1 1 1⟩ crowdion configuration. The most stable clusters are hexagonal in shape with sides along ⟨1 1 2⟩ directions [8,17]. They consist of n successive filled hexagonal shells surrounding a central SIA with a total number N_n of $7, 19, 37, \ldots, N_{n-1} + 6(n-1)$. The absence of jogs on the sides of these clusters contributes to their stability, i.e., the binding energy of the last interstitial that completes the 19 SIAs cluster is either 2.5 eV (vertex) or 3.3 eV (side) whereas the binding energy of the 20th interstitial is either 1.4 eV (vertex) or 1.9 eV (side). Thus clusters tend to these most stable shapes by either growth or shrinkage. The stress field of these clusters is highly anisotropic; there is a compression region extended mainly along the crowdion direction. Fig. 5

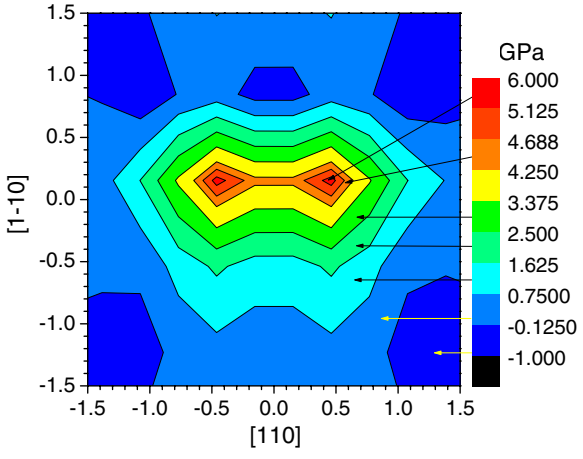

Fig. 4. Pressure map in GPa of a [1 1 0] interstitial in the (0 0 1) plane.

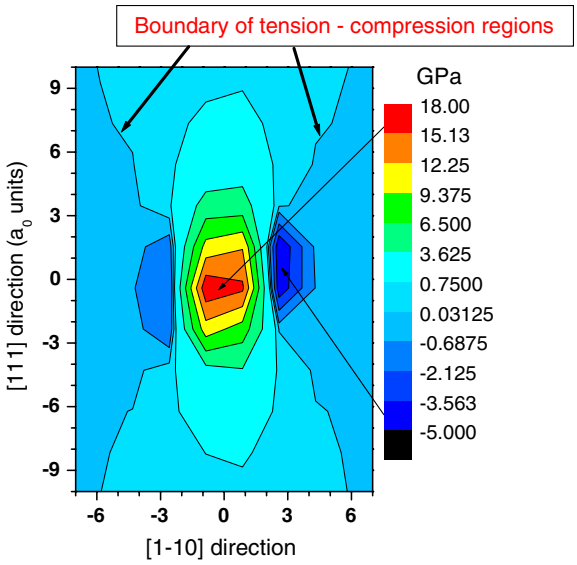

Fig. 5. Pressure map in GPa of the (1 1 −2) cross section of a 19 SIA cluster with (1 1 1) habit plane. The isobar at the tension–compression border is indicated.

shows the pressure distribution in a (1 1 0) cross section passing through the centre of the cluster. In terms of dislocation loops, these clusters are edge loops with Burgers vector 1/2 [1 1 1]; they are mobile and perform a 1D motion along the glide prism [18]. An important characteristic of interstitial clusters in bcc iron is that the crowdions move individually along the crowdion line, giving to the cluster a high mobility; moreover the migration energy is almost independent of the number of SIAs of the cluster for clusters up to few tens of SIAs [19].

Using an earlier potential by Ackland et al. [20] it was shown [10] that the interaction of these clusters with vacancies occurs when vacancies are inside the glide prism, and then the cluster moves towards the vacancy. However vacancies recombine only with the interstitials at the periphery of the cluster. We have reproduced these results using the new Ackland potential [11] and we observed that vacancies located at first neighbour positions near the cluster habit plane also recombine with the interstitials of the periphery. A vacancy located inside the cluster does not recombine but prevents the movement of the cluster until the vacancy migrates to the periphery and recombines. [10]. Thus the interaction with a vacancy is an effective mechanism for the temporal suppression of the cluster mobility.

4. Results

4.1. Interstitial–cluster interaction

We present the binding energy of the two smallest hexagonal clusters of 7 SIAs and 19 SIAs (7C and 19C hereafter) with an interstitial as a function of the interstitial position and interstitial orientation.

4.1.1. Interstitial located inside the cluster glide prism

We describe, in parallel for the two clusters, the interaction when the interstitial is located at lattice positions of the crowdion line either in the centre of the cluster denoted as (0 0 0) (Fig. 6(a) and (b)) or the side of the cluster, namely (1 1 1) for 7C (Fig. 6(c)) and (2 2 −1) for the 19C (Fig. 6(d)). The six curves in each plot correspond to the six orientations of the interstitial. In the legend of all plots of the paper the tree first symbols correspond to the 'inplane' orientations and the other three are the 'outplane' orientations.

Fig. 6(a) and (b) shows that for $Z > 3a_0$ the interstitial has negative binding energy (as expected) and the two groups of overlapping curves indicate that the interaction depends on whether the orientation is inplane or outplane. The energy has a minimum (−0.3 eV) at $Z = 4a_0$ and $5a_0$ for 7C and 19C, respectively, corresponding to the outplane orientations. The difference in the binding energies for the inplane and outplane orientations is an effective driving force for the reorientation of an 'outplane' interstitial by migrating to the nearest position into an 'inplane' orientation. Thus, effectively, the binding energy has a minimum value of −0.05 eV that represents a weak repulsion.

The main differences between the two clusters appear when the interstitial is located at distances $Z < 3a_0$. In the 7C (Fig. 6(a)), all orientations relax into configurations of positive binding energy. In fact the crowdions of the cluster move towards the interstitial and form complexes like the one shown in Fig. 7(a). In the 19C (Fig. 6(b)) three orientations have almost no binding energy whereas the other three ($E^b = 0.4$ eV) relax into a complex like the one shown in Fig. 7(b). This special configuration, with two interstitials in almost perpendicular orientations, appears quite often under the cluster–interstitial interaction study when the interstitial is located close enough to the cluster either inside or outside the glide prism. A similar configuration appears in clusters of 4–5 SIAs that diffuse at $T \geqslant 400$ K as a result of the defocusing of one of its crowdions [21].

Fig. 6(c) and (d) shows the interaction at points located above the side of the cluster. For distances $Z > 3a_0$ the interactions are like those on the line through the centre of the cluster although, since the interstitials are at the edge of the glide prism, the probability that the interstitial jumps out of the cluster glide prism is higher. For distances $Z < 3a_0$ the SIA migrates outside the glide prism, reorients into the [1 1 1] orientation and is absorbed by the cluster forming a new cluster of 20 interstitials. This happens with two orientations for the 7C (1.6 eV) and with four orientations for the 19C, i.e., $E_b = 1.9$ eV if the interstitial is accommodated at the side and $E_b = 1.35$ eV if the interstitial is accommodated at the vertex. Up to $4\Delta z$ in 19C and up to $3\Delta z$ in 7C the interstitial forms the above mentioned complex shown in Figs. 7(a) and 7(b) with 0.85 eV $< E^b$(19-C) $<$ 1.0 eV and 0.7 eV $< E^b$(7C) $<$ 0.8 eV. An inplane SIA at a distance $2a_0 \leqslant Z \leqslant 3a_0$ near the vertex, in both clus-

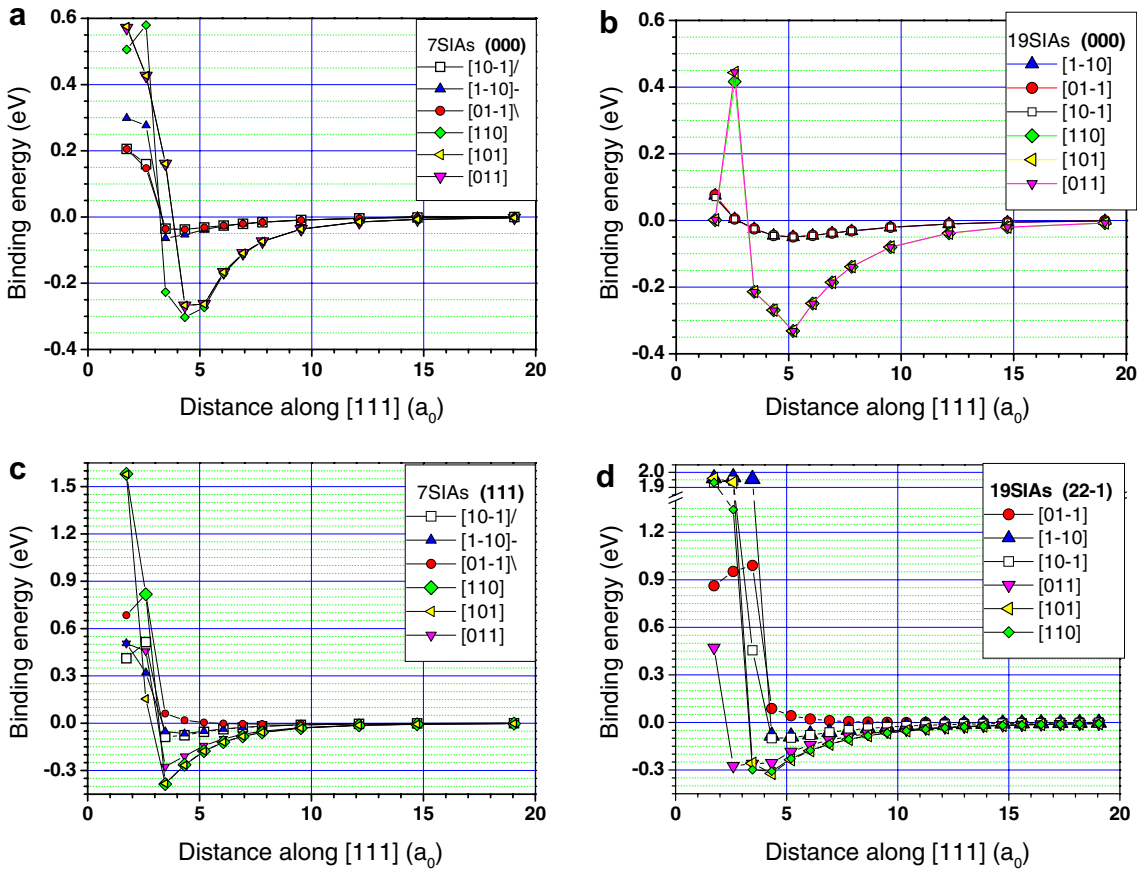

Fig. 6. (a,c) Binding energies of an interstitial with a 7 SIA cluster along a [1 1 1] line (a) through the cluster centre and (c) through the cluster vertex. (b,d) Binding energies of an interstitial with a 19 SIA cluster: (b) through the cluster centre and (d) through the cluster vertex.

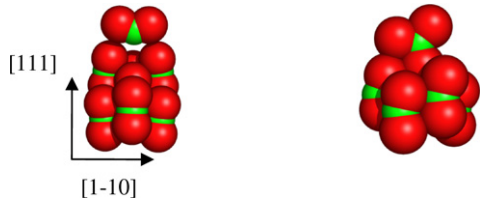

Fig. 7(a). 7 SIAs cluster interacting with an interstitial within the glide prism. The right image shows the complex formed when the interacting interstitial forms a T-shaped complex with one of the crowdions of the cluster.

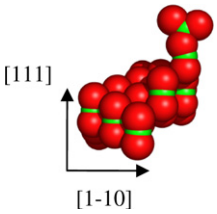

Fig. 7(b). Complex formed by a 19 SIAs cluster plus an interstitial. Notice the displacement of one crowdion from the cluster towards the interacting interstitial to form a T-shaped complex.

ters, presents another special configuration shown in Fig. 7(c) for the 7C. This is a stable configuration, as

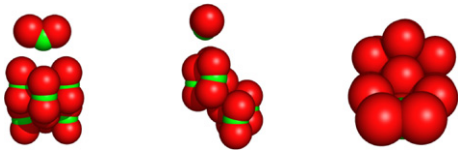

Fig. 7(c). Three views along X, Y and Z directions of a shot taken from the evolution of a 7 SIA cluster interacting with an interstitial inside the glide prism at $T = 100$ K. The interstitial remains inside the glide prism, it keeps the distance to the cluster and jumps to equivalent positions on adjacent vertexes of the cluster.

described in Section 4, and the interstitial can jump from one corner to the next.

4.1.2. Interstitial located outside the cluster glide prism

4.1.2.1. Interstitials located at first neighbour positions. Figs. 8(a)–(d) show the binding energy for interstitials located above the cluster habit plane along [1 1 1] lines passing through the points (3 −3 0) and (3 3 0) for the 19C and the equivalent points (2 2 −1) and (2 −2 1) in the 7C. Comparing the plots labelled (3 3 0) to the (3 −3 0) and the plots labelled (2 2 −1) to the (2 −2 1) we can see that there is no mirror symmetry across the plane $Y = 0$. This general description is valid for the second neighbour positions and third neighbour positions.

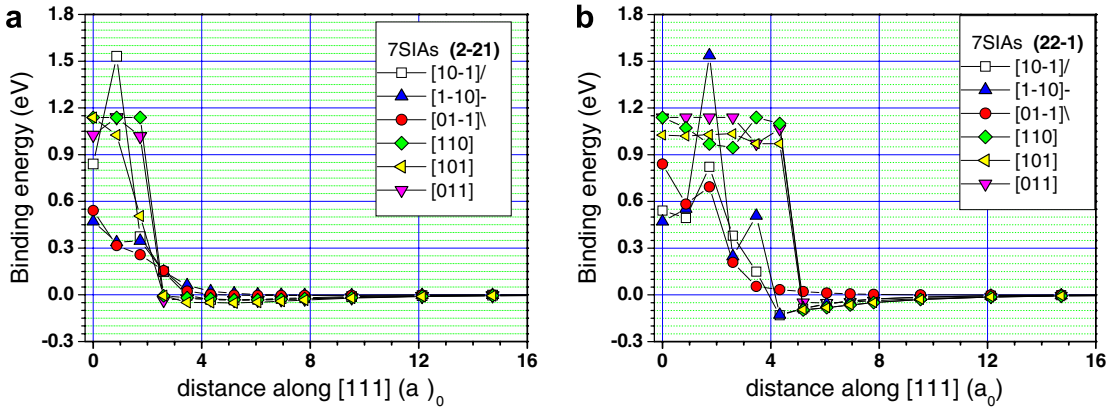

Fig. 8(a,b). Binding energies for the 7 SIAs cluster–SIA interaction along a first neighbour [1 1 1] line through (a) the (2 −2 1) point and (b) the (2 2 −1) point.

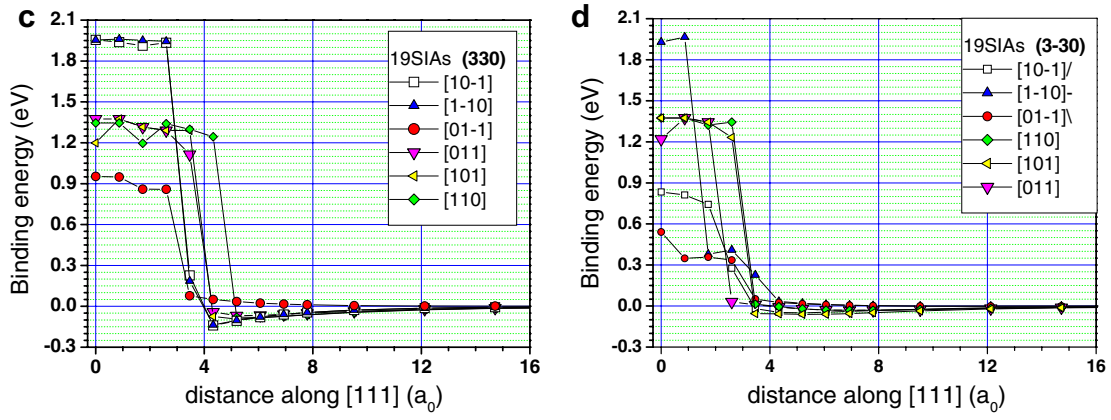

Fig. 8(c,d). Binding energies for the 19 SIAs cluster–SIA interaction along a first neighbour [1 1 1] line through (c) the (3 3 0) point and (d) the (3 −3 0) point.

First neighbour positions are characterized by spontaneous absorption of the interstitial by the cluster. The capture distance of spontaneous absorption, measured from the cluster habit plane to the farthest position where the interstitial may be captured, is $4.5a_0$. For distances $Z \leqslant 5a_0$ the interactions are strongly dependent on the orientation of the interstitial but generally speaking there is attraction and both cluster and interstitial move, i.e., the interstitial migrates by changing orientation and position and the cluster deforms by moving the crowdions that are closer to the interstitial. The final energy balance, namely, the binding energy $E^b(20)$ of the interstitial number 20 of the former 19 SIAs cluster, depends on the final position of the interstitial when it reorients to the crowdion configuration and joins the cluster. A binding energy $E^b(20) = 1.9$ eV and $E^b(8) = 1.5$ eV, for the former cluster of 7 SIAs, indicates that the interstitial has reoriented to the [1 1 1] orientation and has joined the side of the cluster. If $1.0\ \text{eV} < E^b(20) < 1.5\ \text{eV}$ or $0.9\ \text{eV} < E^b(8) < 1.2$ eV the interstitial reorients to [1 1 1] but it is located at the vertex of the cluster. Any other value corresponds to an interstitial that keeps its initial orientation. When the interstitial is located near the cluster (up to $5\Delta z$) the closest crowdions of the cluster move towards it. As a result the cluster is deformed or displaced until it captures the interstitial. Values of the binding energy of the order of 0.9 eV indicate that the corresponding relaxed configurations are sessile complexes like the one shown in Fig. 7(b).

4.1.2.2. Interstitials located at second neighbour positions. The lines passing through (3 3 0) and (4 4 1), among the 4 and 5 different lines at second neighbour positions for 7C and 19C, respectively, are presented in Fig. 9(a) and (b). As in the previous cases, the peculiarities appear at distances to the cluster habit plane $z < 4a_0$ where there is a gradation of positive binding energies from 0.07 eV to 0.5 eV. In these cases the interstitials keep their original orientation but the cluster is deformed due to the local attraction of the nearest crowdions. A small movement of the interstitial would result in its absorption by the cluster.

Thus, at $T > 0$ K the region where the binding energy is of the order of 0.4–0.5 eV is an effective capture zone with a capture distance $Z = 3.5a_0$. Even at $T = 0$ K the interstitial in the [10−1] orientation located at the point (4410) migrates under relaxation to the (336) point, then rotates to the [111] orientation and it is absorbed by the cluster (point with energy 1.3 eV in Fig. 9(b)). In the figure an image of the cluster after the absorption is presented. This absorption also occurs for some orientations of interstitials located at the other second neighbour positions and $Z < 2a_0$. There is no spontaneous absorption for third neighbours and beyond.

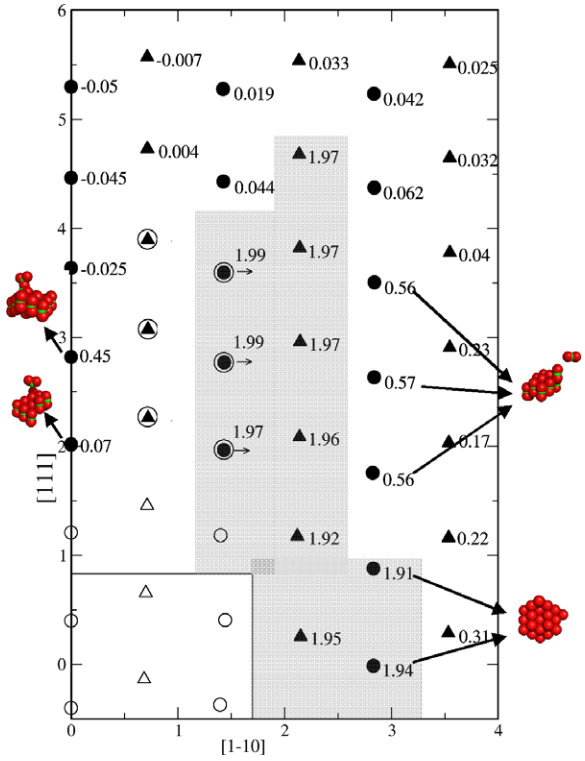

Fig. 9. $(1\,1\,\bar{2})$ cross section of the system through the cluster centre for the 19 SIA cluster (rectangle in the lower left part). The value of the highest binding energy, in eV, according to the interstitial orientation is presented at the lattice sites. The shadowed region indicates the sites where the interstitial is absorbed by the cluster. The axes are in lattice parameters. The sites encircled indicate that the interstitial is unstable and it is ejected outside the cluster glide prism; the corresponding binding energy indicates absorption by the cluster. Examples of each possible final configuration are superimposed.

The maximum interaction distance perpendicular to the cluster including second neighbour positions is about $25a_0$ where the binding energy for inplane orientations is negligible and the binding energy for outplane is smaller in absolute value than 10^{-3} eV.

4.1.3. Interstitial located in the cluster habit plane

To determine the binding energy at the cluster habit plane, the interstitial has been located out of the cluster along three coplanar lines, namely, the X-axis and the sides [1 −2 1] and [2 −1 −1] of the triangle in Fig. 3. As an example, Fig. 10 presents the results along the [1 −2 1] direction for the 19C.

All binding energies are positive as expected in a tensile region of the stress field of the cluster (see Fig. 5). At distances, from the cluster centre, $r \geqslant 4a_0$ the energy decreases smoothly from a maximum value of 0.16 eV–7×10^{-3} eV at $r = 14a_0$. At distances $r > 6a_0$ the value of the binding energy is smaller than 0.05 eV and is independent of the interstitial orientation.

4.1.4. Migration energy barrier of an interstitial in the vicinity of a cluster

In order to calibrate the influence of the cluster stress field in the migration energy barrier, the later has been calculated at several sites of the second neighbour positions. Thus, at a given site the interstitial was moved to the nearest positions and this was repeated for the six orientations. The results proved that the new energy migration barrier satisfy the following empirical approximation: $E_m = E_m(\text{bulk}) - 1/2\ \ (E_b(f) - E_b(i))$, where $E_b(i)$ and $E_b(f)$ are the binding energies of the interstitial at the initial

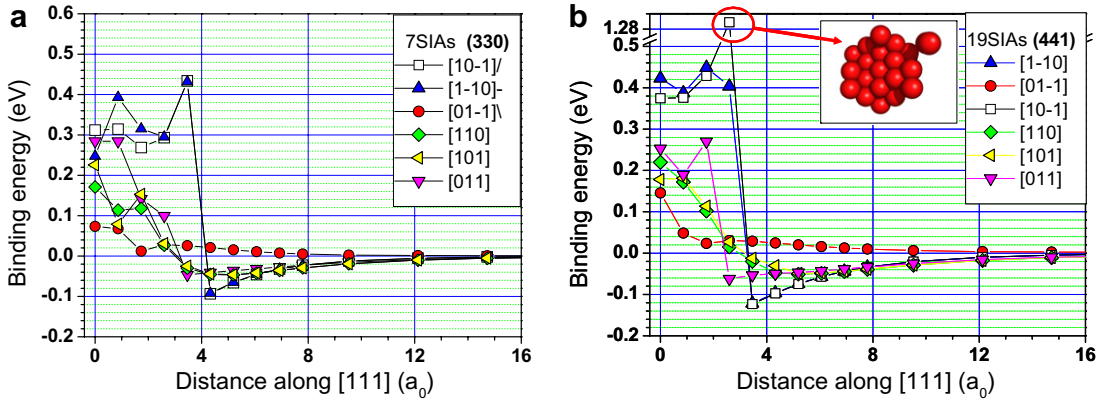

Fig. 10. Binding energies of: (a) the 7 SIA cluster–SIA interaction along a second neighbour [1 1 1] line through the (330) point and (b) the 19 SIA cluster–SIA interaction along a second neighbour [1 1 1] line through the (441) point. The position where there is absorption of the interstitial by the cluster is indicated and the final configuration is superimposed.

and final positions, respectively. Since the binding energy increases going towards the cluster, the barrier is smaller for jumps towards the cluster glide prism which increases the probability of such a jump and further absorption.

4.1.5. Spontaneous absorption of an SIA and comparison with vacancy recombination

The distance of spontaneous absorption of an SIA by a cluster calculated in a static simulation ($T = 0$ K) gives the minimum value of recombination distance. In Fig. 11 we present a $(1\,1\,\bar{2})$ cross section of the system through the cluster centre for the 19C where the region of spontaneous absorption has been shadowed. The cluster centre is located at the origin; two levels of atomic sites are represented by circles ($Y = 0$) and triangles ($Y = \sqrt{6}/4a_0$). At each atomic site the value of the maximum binding energy, relative to the orientation of the interstitial, is indicated. We notice that the sites located above the cluster that are marked with an arrow do not correspond to a direct absorption; the interstitial first jumps to a site out of the glide prism and then joins the cluster. The images of four different relaxed configurations are inserted in the figure at the corresponding sites.

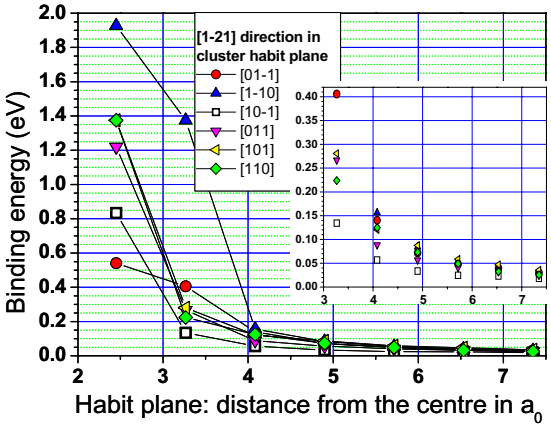

Fig. 11. Binding energies for the 19 SIA cluster–SIA interactions along a $[1\,-2\,1]$ line on the cluster habit plane. The inset shows with more detail the asymptotic values for the different orientations.

The main parameters of the cluster–SIA interaction for 7C and 19C are presented in Table 1 together with the corresponding data for the interaction with a vacancy calculated with the same EAM potential (see Fig. 12(a) for the 19C). The column named 'recombination energy' indicates the energy released to the system when either the interstitial joins the cluster or the vacancy recombines with one of the interstitials of the periphery of the cluster. The region where the point defect is captured is specified in two columns, i.e., by the sites at the cluster habit plane and the distance perpendicular to it. This region is well defined for the vacancy interaction since both, the sites of recombination and the distance undergone by the cluster to meet the vacancy are unambiguously determined. This is not the case for an interstitial since the capture distance depends on the site and on the orientation of the interstitial. Thus, in Table 1 we included the maximum value of the capture distance among the first neighbour positions and the sites with binding energy of the order of 0.5 eV (indicated with $*$) for second neighbour positions.

In Fig. 12 we have included plots corresponding to the binding energy of both vacancy and interstitial in the most favourable case for interaction, namely a vacancy either inside the cluster glide prism or at a first neighbour position (Fig. 12(a)) and an interstitial at a first neighbour position (Fig. 12(b)).

The binding energy for a vacancy is always positive because it is a negative dilatation centre in the compressive part of the stress field of the cluster. The gradient of binding energy is the driving force for the cluster to move towards the vacancy. When the vacancy is aligned with a crowdion of the periphery there is annihilation. The crowdions at the corner release bigger amount of energy because their binding energy with the cluster is smaller than the crowdions at the edge.

The interaction with an SIA is more complex due to the anisotropy of both, the cluster and the interstitial. The binding energy is related, in first approximation, to the component of the stress tensor of the cluster in the direction of the SIA. In the $(3\,1\,1)$ line only one out of six orientations have positive binding energy at all points and the capture distance, $Z = \sqrt{3}a_0$, is the smaller among the capture distances of the other orientations. The points showing

Table 1
Interaction of point defects with 7 SIA and 19 SIA clusters

Cluster interaction with		Recombination energy (eV)	Capture sites in habit plane	Capture distance (a_0) along [1 1 1]
Vac	7C	3.0	All SIAs	4
			1st neighbour	2
	19C	Vertex = 2.8	SIAs at periphery	3.5
		Side = 2.0	1st neighbour	2.5
SIA	7C	1.6	1st and 2nd neighbours	1st neighbour = 4.5
				2nd neighbour = 2*
	19C	Vertex = 1.4	Periphery + 1st and 2nd neighbours	1st neighbour = 4.5
		Side = 1.9		2nd neighbour = 3.5*

Recombination energy indicates the annihilation energy for a vacancy and the absorption energy of a SIA. The effective capture volume is described by the capture sites in habit plane and the distance along the crowdion direction. Distances marked with $*$ are for $T > 0$.

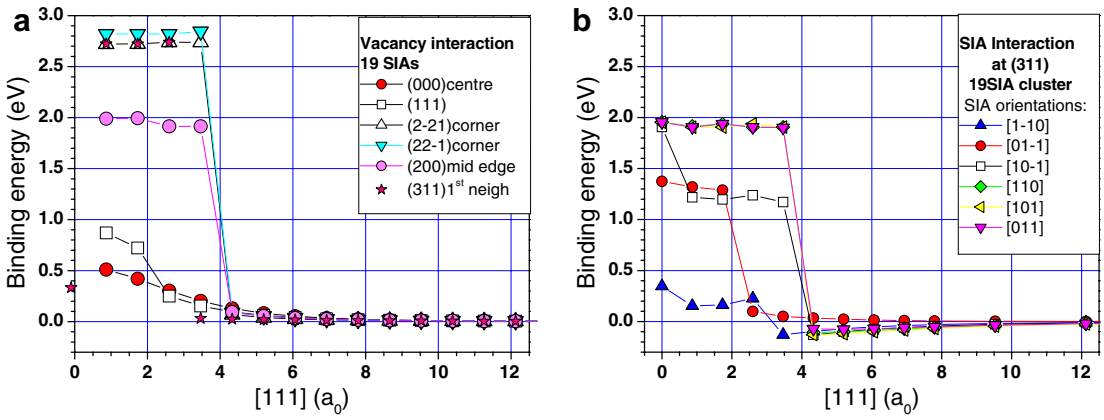

Fig. 12. (a) 19 SIA cluster–vacancy binding energy. Each curve corresponds to the positions along a [1 1 1] crowdion line inside the cluster habit plane; the star symbol corresponds to a [1 1 1] line at a first neighbour position. (b) 19 SIA cluster–SIA binding energy for a SIA located at a first neighbour position; each curve corresponds to a different interstitial orientation.

recombination are points where the equilibrium is unstable, i.e., positive binding energy that allowed the cluster to approach the interstitial and the later to move to a closer position and to rotate to the [1 1 1] orientation necessary for joining the cluster. The SIA migration is trigged by the stress field of the cluster and therefore is dependent on the orientation of the interstitial. The torque applied by the cluster stress field to an interstitial with an orientation 'outplane' is higher than that applied to an interstitial 'inplane' and may be more effective, as indicated by the bigger capture distance of the orientations 'outplane' shown in Fig. 12(b) and in Fig. 8 (4th–6th symbols in the legend).

An important difference between the interaction of SIAs and vacancies is the probability of recombination for $T > 0$ K. The probability of annihilation of a vacancy within the cluster glide prism at a distance of about 8–$10a_0$ is almost 100%. This is because the vacancy does not move during the time that the cluster needs to meet it and, once the vacancy is in the cluster habit plane, the positive gradient of binding energy towards the periphery enhances a fast diffusion of the vacancy to the periphery where it recombines.

The probability for an SIA in a first or second neighbour position at the same distance is much smaller since the binding energy is negative for some orientations and the interstitial can run away before the cluster reaches the recombination distance.

4.2. Checking the stability by MD simulation

There are some configurations of the cluster–interstitial interaction that have been studied by MD simulation to investigate the metastable situations. There are essentially two cases, i.e., when the interstitial is close enough to modify the shape of the cluster and when the interstitial is inside the glide prism of the cluster. We allowed the system to evolve from these configurations at 50 K and 100 K for few nanoseconds in order to allow it to escape from shallow minima of potential energy. In addition some T-shaped configurations have been annealed at 300 K.

We observed that the interstitial located inside the glide prism at distances of about 2–$3a_0$ from the cluster habit plane and oriented inplane tends to stay near a vertex (see Fig. 7(c) for the 7 SIAs cluster) and move from one vertex to the next for few tens of nanoseconds at 100 K until it jumps out of the glide prism, changes into an outplane orientation and finally joins the cluster. During the time that the interstitial is inside the glide prism, the crowdions can jump individually forward and backward but the centre of mass of the cluster does not move.

Similarly, T-shaped structures like the one in Fig. 7(b) last for at least more than a few nanoseconds at 300 K and prevent the cluster motion. Thus, the general situation is that dumbbell interstitials located inside the glide prism inhibit the cluster motion before they can jump to a site out of the glide plane. Thus, this is a possible mechanism to suppress temporally the movement of the cluster.

The absorption of interstitials located at second neighbour lines is dependent on the orientation and was found to happen at positions $Z < 3.5a_0$. At larger separation distances the cluster is slightly inclined towards the interstitial but both defects are stable at $T = 50$ K. Further absorption by the cluster would require the migration of the interstitial.

Few MD simulations at $T = 600$ K with an interstitial either inside or outside the cluster glide prism at distances of 6–$7a_0$ have evidenced that the interstitial can approach the cluster and join it or move away from it. Thus, a statistical treatment is necessary for the study of the interstitial capture efficiency of clusters.

5. Concluding remarks

The interaction of an interstitial with small interstitial clusters of perfect hexagonal shape has been studied and the values of the binding energy for the interstitial at a site either inside or outside the glide prism of the cluster are

presented. A complete set of data for clusters of 7 and 19 SIAs is now available for studies, at the mesoscopic scale, of the evolution of defects produced during irradiation of α-Fe.

The cluster–SIA interaction depends on the position of the interstitial as well as its orientation. If the interaction is attractive, the cluster moves towards the interstitial along its glide prism. Simultaneously, the interstitial migrates and reorients into the [1 1 1] crowdion and joins the cluster. Sometimes, before the reorientation, the interstitial forms a sessile complex with one of the crowdions of the cluster that is stable at low temperature for few nanoseconds.

An interstitial located inside the glide prism of the SIA cluster parallel to the cluster habit plane suffers repulsion at distances $Z > 3a_0$ but has positive binding energy at closer distances, thereby forming complexes that inhibit temporally the cluster motion.

Both the 7 SIA and 19 SIA clusters exhibit the same qualitative behaviour in relation to the interaction with an interstitial outside the glide prism of the cluster. This interaction is attractive at distances smaller than $4–5a_0$ with a binding energy strongly dependent on the orientation of the interstitial. At these distances the cluster is deformed since the closest crowdions move towards the interstitial. For distances from the cluster habit plane $z > 5a_0$ the interstitial has negative binding energy except for one orientation. The interaction does not affect the shape of the cluster but the stress field of the cluster modifies the migration energy barrier of the interstitial that can be approximated by $E_m = E^m_{bulk} - 1/2\ (E^b(f) - E^b(i))$. This implies that the barrier is smaller for jumps towards the cluster glide prism, where $E^b(f) > E^b(i)$ increasing the probability of such a jump and further absorption.

The interaction of the 19 SIA cluster with a vacancy has been included for comparison. It follows some general conclusions on the interaction cluster–point defect.

The interaction with both point defects is produced in the vicinity of the cluster glide prism. A rough estimation of the recombination volume obtained with the data from static simulations ($T = 0$ K) gives a bigger volume for the interaction with the interstitial, i.e., ratios of 2.3 and 1.7 for the 7 SIA and 19 SIA clusters, respectively. These values would indicate a tendency of growing for small clusters. But this estimation does not consider either the different mobility of the three defects or the fact that the vacancy has positive binding energy at all positions inside the cluster glide prism but the interstitial has negative binding energy for many positions and orientations. Thus, the effective recombination volume for vacancies increases at $T > 0$ K whereas it is not clear the kinetics of the interaction with interstitials. A further study based on kinetic Monte Carlo simulation that uses as input the data presented here is needed and it is now in progress.

Acknowledgements

We are grateful to Professor D.J. Bacon, University of Liverpool, for helpful advice, discussions and for the revision of the manuscript. We also acknowledge the numerous discussions with Dr Yu.N. Osetsky, Oak Ridge National Laboratory, and Dr A. Barashev, University of Liverpool. We acknowledge the support of the UE: (PERFECT; FI6O-CT-2003-508840) and the Spanish MEC (FIS2006-12436-C02-02). The calculations were performed in CESCA (Centre de Supercomputació de Catalunya: www.cesca.es).

References

[1] F. Gao, D.J. Bacon, Yu.N. Osetsky, J. Nucl. Mater. 276 (2000) 213.
[2] B.N. Singh, A.J.E. Foreman, Philos. Mag. A 66 (1992) 975.
[3] B.N. Singh, A.J.E. Foreman, H. Trinkaus, J. Nucl. Mater. 249 (1997) 103.
[4] B.N. Singh, S.I. Golubov, H. Trinkaus, A. Serra, Yu.N. Osetsky, A.V. Barashev, J. Nucl. Mater. 251 (1997) 107.
[5] Yu.N. Osetsky, D.J. Bacon, F. Gao, A. Serra, B.N. Singh, J. Nucl. Mater. 283–287 (2000) 784.
[6] Yu.N. Osetsky, D.J. Bacon, A. Serra, B.N. Singh, S.I. Golubov, J. Nucl. Mater. 276 (2000) 65.
[7] Yu.N. Osetsky, D.J. Bacon, A. Serra, B.N. Singh, S.I. Golubov, Philos. Mag. A 83 (2003) 61.
[8] Yu.N. Osetsky, A. Serra, B.N. Singh, S.I. Golubov, Philos. Mag. A 80 (2000) 2131.
[9] M. Pelfort, Yu.N. Osetsky, A. Serra, Philos. Mag. Lett. 81 (2001) 803.
[10] M.A. Puigvi, A. Serra, N. de Diego, Yu.N. Osetsky, D.J. Bacon, Philos. Mag. Lett. 84 (2004) 257.
[11] G.J. Ackland, M.I. Mendelev, D.J. Srolovitz, S. Han, A.V. Barashev, J. Phys.: Condens. Matter 16 (2004) S2629.
[12] Chu-Chun Fu, F. Willaime, P. Ordejón, Phys. Rev. Lett. 92 (2004) 175503.
[13] V.G. Kapinos, Yu.N. Osetsky, P.A. Platonov, J. Nucl. Mater. 173 (1990) 229.
[14] Warren L. DeLano, The PyMOL Molecular Graphic System. DeLano Scientific LLC, San Carlos, Ca, USA. <http://www.pymol.org>.
[15] C. Fu, F. Willaime, Phys. Rev. Lett. 92 (2004) 175503.
[16] F. Willaime et al., Nucl. Instrum. and Meth. B 228 (2005) 92.
[17] B.D. Wirth, G.R. Odette, D. Maroudas, G.E. Lucas, J. Nucl. Mater. 276 (2000) 33.
[18] Yu.N. Osetsky, D.J. Bacon, A. Serra, Philos. Mag. Lett. 79 (1999) 273.
[19] Yu.N. Osetsky, A. Serra, V. Priego, Mater. Res. Soc. Symp. Proc. 527 (1998) 59.
[20] G.J. Ackland, D.J. Bacon, A.F. Calder, T. Harry, Philos. Mag. A 75 (1997) 713.
[21] N. Anento, Yu.N. Osetsky, A. Serra, unpublished work.